Proceedings of the ASME 2009 International Design Engineering Technical Conferences & Computers and Information in Engineering Conference
IDETC/CIE 2009
August 30 - September 2, 2009, San Diego, California, USA

DETC2009-87355

AN ELASTIC EXOSKELETON FOR ASSISTING HUMAN RUNNING

Michael S. Cherry, Sridhar Kota
Department of Mechanical Engineering
University of Michigan
Ann Arbor, Michigan 48105
Email: mscherry@umich.edu

Daniel P. Ferris
School of Kinesiology
University of Michigan
Ann Arbor, Michigan 48109
Email: ferrisdp@umich.edu

ABSTRACT

This paper presents the design and preliminary evaluation of an elastic lower-body exoskeleton. Human legs behave in a spring-like fashion while running. We selected a design that relied solely on material elasticity to store and release energy during the stance phase of running. The exoskeleton included a novel knee joint with a cam and a Bowden cable transferring energy to and from a waist-mounted extension spring. We used a friction-lock clutch controlled by hip angle via a pneumatic cylinder to release the cable during swing phase for free movement of the leg. The design also incorporated a composite leaf spring to store and release energy in the distal portion of the exoskeleton about the foot and ankle. Preliminary test data for our target subject showed that his typical leg deflection was 0.11 m with leg stiffness of 16 kN/m while running at 3.0 m/s. We used these values to set the desired stiffness (60%±15% of the normal leg stiffness, or 9.6±2.4 kN/m) and deflection (0.11 m) of the exoskeleton. We created simplified multi-body and full finite element quasi-static models to achieve the desired system stiffness and validate our results, respectively. The final design model had an overall stiffness of 7.3 kN/m, which was within the desired range. We fabricated a single-leg prototype of the exoskeleton that weighed 7.1 kg. We tested the exoskeleton stiffness quasi-statically and found a stiffness of 3.6 kN/m. While running, the exoskeleton provided ∼30% of the total leg stiffness for two subjects. Although the stiffness was lower than desired, the fabricated prototype demonstrated the ability of a quasi-passive exoskeleton to provide a significant portion of an individual's leg stiffness while running.

1 INTRODUCTION & BACKGROUND

Locomotion is central to people's ability to function independently in their daily lives. Able-bodied individuals take for granted their ability to move about as they perform daily tasks. Individuals with disabilities that affect their locomotive capacity are well aware of the challenges. In a way all individuals are limited in their locomotive capacity. For example we are all bounded by the speeds we can run and the distances we can walk while carrying heavy loads.

Our broad research aim is to develop wearable mechanisms (exoskeletons) for assisting human locomotion, benefitting both able-bodied and individuals with disabilities. For example, those who are able-bodied could run farther at the same speed before becoming fatigued with the addition of an exoskeleton. This would be highly beneficial in either military or search and rescue operations where it is critical to traverse large distances quickly and over rough terrain. An exoskeleton that reduced loads required by specific muscle groups in the leg could also benefit individuals with disabilities, such as muscle atrophy in the lower limb, restoring their locomotive ability. For example, an individual with an atrophied quadriceps muscle group could use an elastic exoskeleton to provide a knee extension (straightening) torque while walking and running, decreasing the demands on existing muscles and enabling locomotion at higher speeds and with greater comfort. Decreasing loads at specific joints in the lower limb may prove beneficial for individuals suffering from osteoarthritis. A leg exoskeleton capable of sustaining a portion of an individual's body weight would decrease the bone on bone forces at the joints and decrease pain while enabling locomotive

ability. In this sense the elastic exoskeleton could take on the role of a body-weight support system that does not need to be used in a laboratory environment. Typical body-weight support systems are large, bulky and not suitable for daily use. Development of a lightweight low-profile wearable exoskeleton that supports a significant portion of body weight could be used for locomotion rehabilitation in the wearer's home and natural surroundings.

1.1 Literature Review

The most well-publicized exoskeletons in mass media are highly complicated and energy intensive wearable robots (Berkeley [1], Cyberdyne [2], and Sarcos [3]). These robots are designed to augment human capability through active mechanical power generation via motors and actuators. In general, they do not make use of elastic components to store and release energy during locomotion. In contrast, humans make excellent use of elastic energy storage and return during both human walking and running (see [4], [5], and [6]).

Only a handful of devices have been designed to incorporate elasticity, decreasing the demands on actuators while enabling simpler designs. One method for including elasticity is through series elastic actuators. The RoboWalker [7] and the powered exoskeleton developed by Low et al. [8] use this method. Walsh et al. developed an alternate method of incorporating elasticity [9] in which elastic elements were placed at the hip and ankle joints in an exoskeleton designed to carry heavy loads. A variable-damper was used at the knee in this design, resulting in small but significant power-consumption by the device. Carr and Newman implemented the same variable damper in a leaf-spring-based elastic leg exoskeleton to model and understand locomotion by astronauts in space suits [10]. Banala developed an entirely passive elastic exoskeleton [11] based on principles of gravity balancing [12]. Dollar and Herr designed a quasi-passive knee exoskeleton for use while running but have only published results from bench tests thus far [13]. The device by Dollar and Herr is the most similar to the work presented in this paper. A more complete review of exoskeletons and orthoses for assisting human locomotion can be found in [14].

1.2 Summary

The objective of the research presented in this paper was to simulate, design, fabricate, and test an elastic exoskeleton for assisting human running. The design we present in this paper depends solely upon material elasticity to store and release energy during locomotion while supporting the weight of the user. The only energy required to operate the device is used for controlling a friction-lock clutch. This clutch enables switching between stiff and compliant states for the stance and swing phases of running, respectively. The design also aims to be a low-profile exoskeleton, matching the motion of the legs without encumbering their mobility.

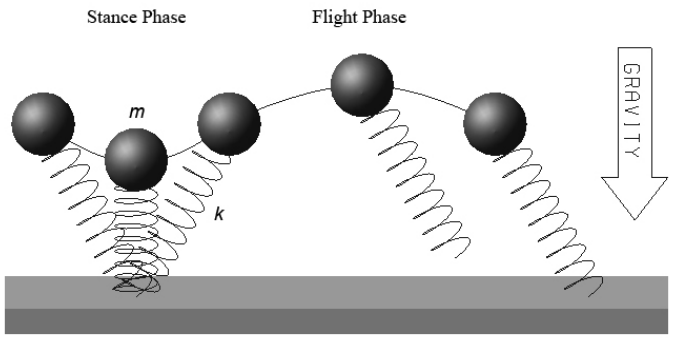

Figure 1. SPRING-MASS MODEL FOR RUNNING. m—POINT MASS, k—SPRING CONSTANT REPRESENTING LEG STIFFNESS. THIS MODEL ACCURATELY DESCRIBES THE CENTER OF MASS MOTION AND GROUND REACTION FORCES FOR BOUNCING GAITS. THIS DEPENDENCE ON ENERGY STORAGE VIA ELASTIC MECHANISMS WAS THE PRIMARY REASON FOR SELECTING RUNNING AS THE APPLICATION OF OUR ELASTIC EXOSKELETON. ADAPTED FROM [16].

2 DESIGN PROCEDURE

The simplest model for running includes a spring representing the function of the legs and a point mass representing body mass (see Fig. 1, [15], [16], and [17]). Human walking dynamics can also be explained using a spring-mass model (see [18] , [19], [20], and [21]). During walking, however, leg deflections are smaller and play a lesser role in the overall energetics of the system compared to running. Consequently an elastic leg exoskeleton would likely be more effective for running, which will be the focus for our design.

2.1 Setting Design Requirements

We tested a single subject running on a force-plate mounted treadmill to collect information about design parameters for the exoskeleton. Visual markers were attached to the lower limbs and torso to record body motion. Trials were conducted at three different speeds (2.6, 3.0, and 3.4 m/s) and in two running conditions, running with heel-strike and running on the balls of the feet (toe running). Data was similar for all trials. The results presented and used for setting design requirements are taken from the 3.0 m/s toe-running trials.

We used two visual markers to define connection points of the exoskeleton to the subject near the lateral iliac crest (hips) and the fifth metatarsal head (foot). We calculated the desired length of the exoskeleton by taking the norm of the vector between these two markers. We calculated the portion of the ground reaction force that would be directed along the exoskeleton by taking the dot product of the direction vector with the ground reaction force vector during stance. These results are provided in Figs. 2 and 3

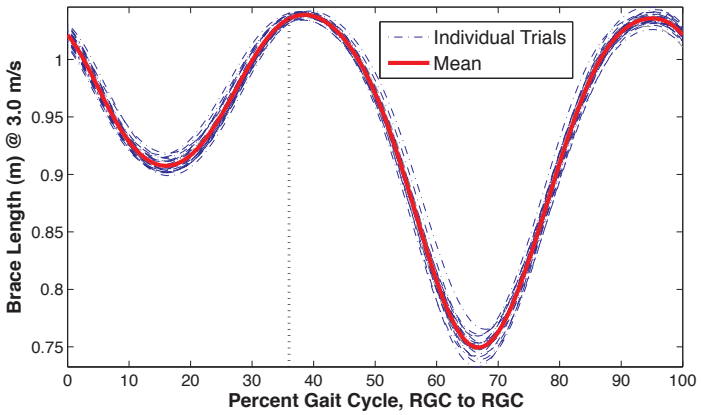

Figure 2. LENGTH OF VECTOR BETWEEN PROPOSED ATTACHMENT POINTS NEAR LATERAL ILIAC CREST AND FIFTH METATARSAL HEAD. THE HORIZONTAL AXIS REPRESENTS PERCENT STRIDE CYCLE, STARTING AND ENDING AT RIGHT GROUND CONTACT (RGC). THE VERTICAL DOTTED LINE REPRESENTS RIGHT TAKE-OFF (RTO).

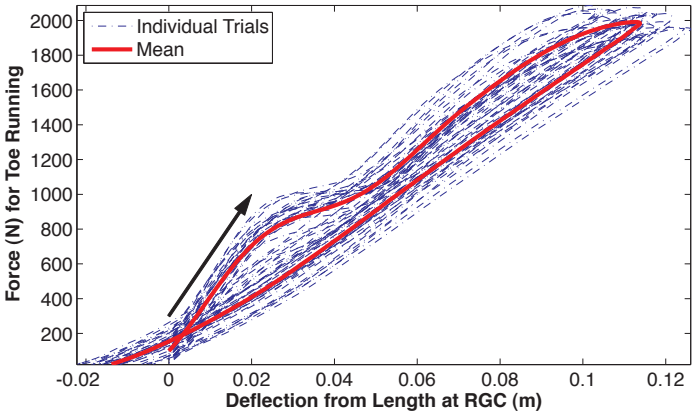

Figure 3. PORTION OF GROUND REACTION FORCE DIRECTED ALONG PROPOSED EXOSKELETON. THE HORIZONTAL AXIS REPRESENTS DEFLECTION OF THE PROPOSED EXOSKELETON FROM THE INITIAL LENGTH AT GROUND CONTACT. THE ARROW INDICATES DIRECTION OF FORCE DEVELOPMENT.

respectively.

We set length specifications from the length data and determined the desired stiffness by calculating the linear least squares fit through the mean force-deflection curve shown in Fig. 3. The desired exoskeleton stiffness was approximate because there was large variability in leg stiffness. Consequently it was not critical to have an exact value for the exoskeleton stiffness, but was sufficient to have it in a reasonable range. Previous designs of elastic orthoses for hopping (see [22] and [23]) demonstrated that an orthosis with 30-50% of the relevant joint's stiffness allows for meaningful decreases in muscle activation without becoming uncomfortable or excessively perturbing the user's kinematics. In these designs it was also noted that much of the stiffness provided by the orthoses was lost at the interface between the orthoses and the human subjects (e.g. soft-tissue deformation). To compensate for this loss in stiffness the target stiffness should be increased by approximately 50%. Consequently, to achieve the desired 30-50% effective stiffness we set the design specification for exoskeleton stiffness at 45-75% leg stiffness, or 60$\pm$15%. The design specifications are summarized in Tab. 1.

2.2 Conceptual Design

During the concept generation phase over a dozen concepts were considered and evaluated. The desired attributes for the exoskeleton were as follows: lightweight, minimal moving mass on the legs, low-profile (closely matches the shape of the leg during all phases of the stride cycle), quasi-passive (relying solely on elastic mechanisms to store and release energy while running), and robust to variations in the users kinematics as well as adjustable to variations between users. The top five concepts were ranked according to these criteria using Pugh charts and a final concept was selected. Due to the space requirements these various concepts and their ranking are not presented in this paper. Rather, we focus on the design that was selected as the best candidate.

2.2.1 The Knee Disk In this concept (see Fig. 4) the leg exoskeleton would attach to the hips of the wearer by a conventional spherical joint. A lightweight rigid structure (e.g. hollow tube) would extend from the hip joint to the general area of the knee. Although this segment would lie in close proximity to the thigh, it would not be attached so as not to constrain the motion of the leg. This rigid segment would connect with a revolute joint to the compliant segment that would extend from the end of this rigid link down to the ball of the foot near the fifth metatarsal head. The compliant segment would also rigidly attach to a pulley (knee disk, or cam) over which a cable would be routed.

This Bowden cable would remotely control the state of the

Table 1. DESIGN SPECIFICATIONS FOR THE ELASTIC EXOSKELETON BASED ON PRELIMINARY RUNNING DATA.

Description	Value
Initial exoskeleton length	1.02 m
Exoskeleton deflection under load	0.11 m
Approximate exoskeleton stiffness	9.6$\pm$2.4 kN/m

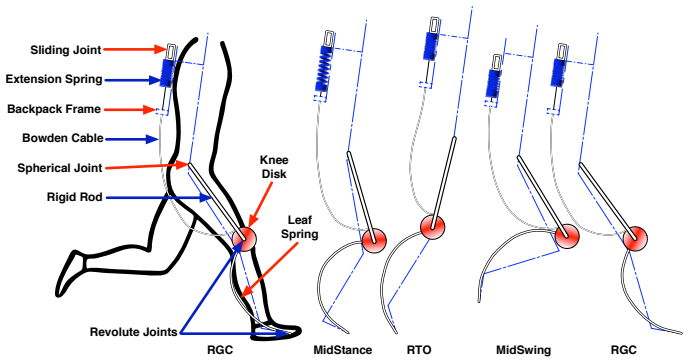

Figure 4. CONCEPTUAL DESIGN FOR AN ELASTIC LEG EXOSKELETON EXTENDING FROM THE HIPS TO THE FOOT. COMPLIANCE IS INCLUDED VIA THE LEAF SPRING EXTENDING FROM THE KNEE REGION TO THE FOOT AND AT THE EXOSKELETON KNEE BY MEANS OF AN EXTENSION SPRING AND A BOWDEN CABLE. THIS CABLE SYSTEM IS ALSO THE MEANS WHEREBY THE SYSTEM IS ALLOWED TO MOVE FREELY DURING SWING PHASE AND LOCK DURING STANCE PHASE TO PROVIDE THE DESIRED STIFFNESS. COMPONENTS ADDRESSED IN THE DETAILED DESIGN STAGE ARE LABELED.

leg exoskeleton. When the cable moves freely (MidSwing in Fig. 4) the leg sections would bend at the joint between the rigid upper and compliant lower segments. When the cable is held taut (MidStance in Fig. 4) the compliant segment would compress to store energy while the knee joint would also bend, storing energy in the extension spring attached to the other end of the cable. This energy would build up during the first half of stance and then release as the user progresses towards push-off. In essence, the knee disk in conjunction with the extension spring located on the back of the wearer would act as a torsion spring at the knee without having to place the mass of a torsion spring there. As the foot leaves the ground the sliding joint on the back releases and the user could freely move their leg during the swing phase. The sliding joint could be controlled by a variety of means including a variable damper, ratchet-pawl mechanism, or friction lock clutch.

This concept would allow for relatively little mass on the legs and a robust method for transitioning the exoskeleton between stance and swing phase configurations. This design would also match the shape of the leg quite closely throughout the running stride cycle. The major disadvantage to this design was that the spring located on the back would increase the total mass of the device. The impact of this was acceptable since the weight would be attached to the trunk where it would be the least costly to carry from a metabolic perspective [24].

2.3 Detailed Design

The overarching goal of the detailed design phase was to select dimensions for all components such that the design would achieve a relatively low weight with acceptable exoskeleton stiffness and factors of safety. Of secondary importance we desired to keep the exoskeleton low profile throughout the stride cycle. To this end we attempted to minimize the diameter of the knee disk and constrain the maximum knee disk rotation during stance. Preliminary testing indicated that the knee underwent 30 degrees of rotation during the stance phase of running. In order to keep the exoskeleton low profile during the stance phase we sought to have the exoskeleton knee joint undergo a similar rotation. However, the amount of rotation did not need to match exactly since the exoskeleton did not attach to the user's leg near the knee.

In this exoskeleton design the user does not feel the effects of the knee spring separately from the lower-leg leaf spring. Rather, the overall stiffness of the exoskeleton is felt by the user as a force on the joint connecting the rigid rod to the hip harness. The two elastic components combined provide the desired stiffness. Consequently, it was necessary to choose the diameter of the knee disk in conjunction with selecting the extension spring stiffness and the stiffness for the lower-leg leaf spring. This required a system model that captured the effects of all three values.

2.3.1 System Modeling In the system model the leaf spring was modeled as a linear compression spring and the knee disk/extension spring combination was modeled as a torsion spring at the knee. A screenshot of this model is shown in Fig. 5. In the physical system when the leaf spring compresses the top of the spring rotates unlike the top of the idealized compression spring. To compensate for this rotation a dummy body representing the knee disk was created and a coupler caused it to rotate relative to the compression spring as the spring compressed. The rate at which it rotated as well as the stiffness of the spring itself was extracted from a finite element model of the leaf spring (see Fig. 6). In the leaf spring model a 3.6 cm displacement directed along the line between the two revolute joints was imposed at the top while the joints at the bottom were pinned to ground.The reaction force required to cause the deflection and resulting knee joint rotation were measured. The resulting stiffness curve and coupling of rotation to compression are shown in Figs. 7 and 8 respectively.

2.3.2 Comparison of ADAMS System Model to Full Finite Element Model In order to verify that the multibody ADAMS system model was accurate we created the equivalent model in ANSYS. In this model the thigh rod was modeled as a solid steel rod such that it underwent negligible deformation. The leaf spring was the same as the one used in the previous section. The upper link and the leaf spring were connected with a

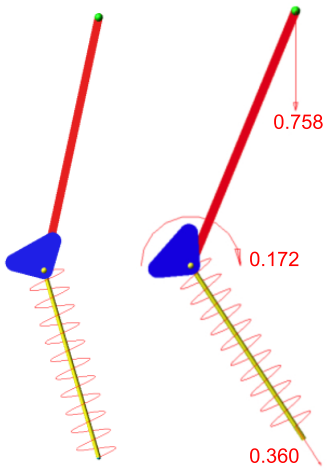

Figure 5. ADAMS MODEL OF THE EXOSKELETON SYSTEM. A TORSION SPRING AT THE "KNEE" REPRESENTS THE STIFFNESS OF THE EXTENSION SPRING ON THE USER'S BACK AND KNEE DISK COMBINED. THE LOWER-LEG LEAF SPRING WAS MODELED AS A COMPRESSION SPRING. A COUPLER PROVIDED THE CORRECT KNEE DISK ROTATION AS THE LEAF SPRING COMPRESSED. VALUES FOR THE COMPRESSION SPRING STIFFNESS AND ROTATIONAL COUPLER WERE CALCULATED FROM A FINITE ELEMENT MODEL OF THE LEAF SPRING (Fig. 6). FORCES (IN kN) AND TORQUES (IN kN-m) SHOWN ARE FOR THE MAXIMUM DEFLECTION OF 11 cm.

revolute joint and a torsion spring as in the ADAMS model. The leaf spring was connected to ground with revolute joints as before. An 11 cm displacement was applied to the top of the upper rod while it was able to rotate freely about the x-axis, the same axis as the other revolute joints. This model is shown in Fig. 9 while Fig. 10 shows the resulting ground reaction forces, knee disk rotations, and leaf spring deformations for both the simplified multi-body model and the full finite element model.

These plots show that the two models agreed with a relatively high degree of accuracy. There was some discrepancy between the two models that is easily explained by simplifications involved in the ADAMS model. Specifically, the finite element model of the leaf spring only had an applied displacement whereas the physical system and full finite element model have applied forces and torques at the knee joint. The applied displacement estimated the force accurately, but could not provide a torque. Although this discrepancy was significant, the error introduced by making this simplification was minimal (see Fig. 10). Consequently, we were confident that the model remained sufficiently accurate for design purposes.

Another reason for the discrepancy was out-of-plane effects present in the ANSYS model but neglected in the ADAMS model. The ADAMS model assumed that the leaf spring behaved

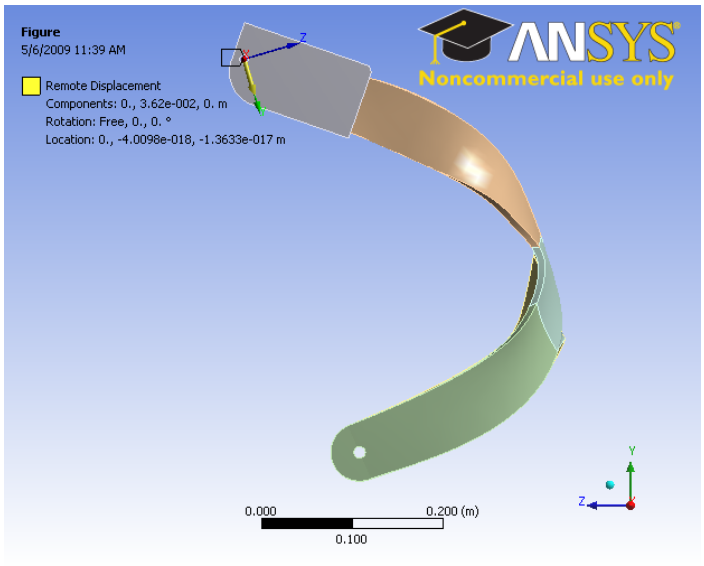

Figure 6. FINITE ELEMENT MODEL OF CARBON COMPOSITE LOWER-LEG LEAF SPRING. THIS MODEL WAS USED TO CALCULATE IDEALIZED VALUES FOR THE MULTI-BODY ADAMS MODEL.

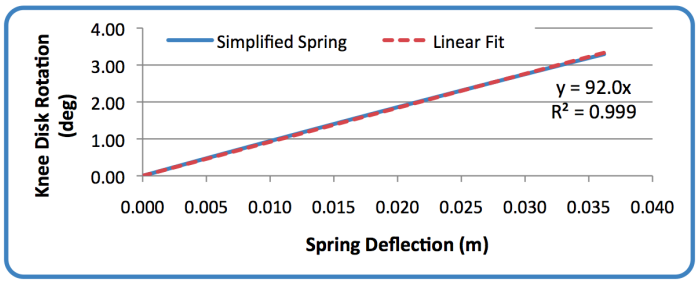

Figure 7. ROTATION OF THE TOP OF THE LEAF SPRING AS IT IS COMPRESSED. BEST-FIT LINEAR SLOPE WAS USED AS A ROTATIONAL COUPLER IN THE ADAMS MODEL.

as a simple compression spring that could not buckle out of plane due to revolute joints at both the top and bottom of the spring. In the finite element model the leaf spring was allowed to buckle and twist which provided some reaction torques to the upper and lower connections of the spring. The leaf spring had two revolute joints at its lower end and a revolute joint connecting the leaf spring to the thigh segment. Because of this the exoskeleton leg did not buckle out of plane even though it was given that degree of freedom in the full finite element model. At the full 11 cm vertical hip deflection the maximum out-of-plane deflection at the knee joint was a negligible 0.14 cm.

All finite element models were constructed in ANSYS Workbench with Solid186 elements. These are 20-node elements and the vast majority of them were quadratic. A small number of

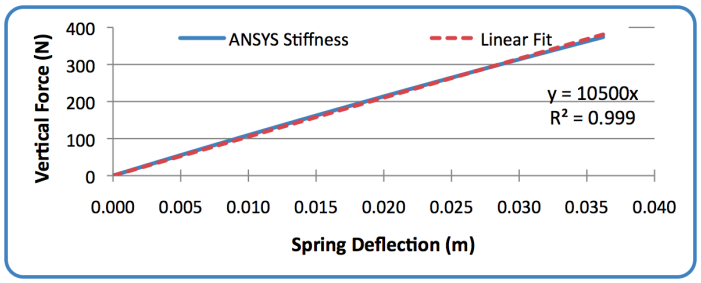

Figure 8. REACTION FORCE REQUIRED TO COMPRESS SPRING THROUGH THE APPLIED DEFLECTION. BEST-FIT LINEAR SLOPE WAS USED AS THE COMPRESSION SPRING STIFFNESS IN THE ADAMS MODEL.

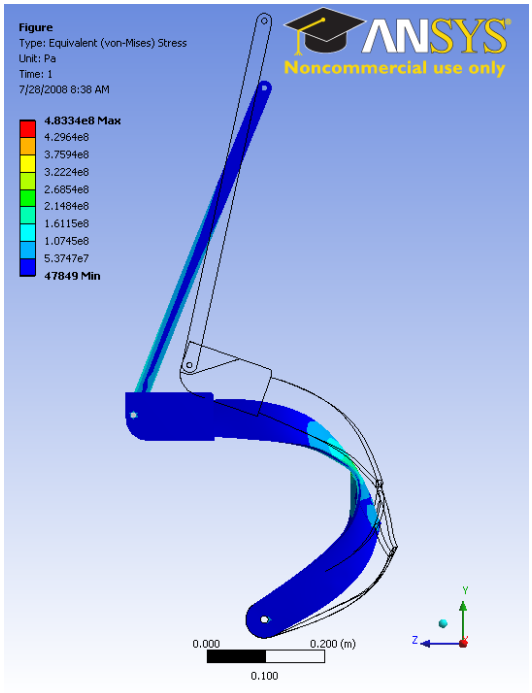

Figure 9. FINITE ELEMENT MODEL OF THE EXOSKELETON LEG SYSTEM USED TO VALIDATE THE SIMPLIFIED ADAMS MODEL.

tetrahedral and wedge elements were also used, e.g. to maintain proper shape of the elements in areas of large curvature or abnormal shape. The mesh density was chosen in order to guarantee at least two elements through the thickness of the smallest dimension in the parts. This provided adequate resolution of bending stresses throughout the model.

2.3.3 Elastic Elements Using the ADAMS model, we first went about determining the desired values for the torsion spring and leaf spring stiffnesses. In order to simplify the selection of parameters for the lower-leg leaf spring only two design variables were used, the cross-sectional thickness and width. This constant cross-section was used throughout the leaf spring. The design variables for the torsion spring were the extension spring stiffness and the knee disk diameter. We varied these four values until a combination was achieved resulting in approximately 30 degrees of knee disk rotation and overall exoskeleton stiffness in the range of 9.6±2.4 kN/m. The values of these variables and the resulting design objectives are provided in Tab. 2.

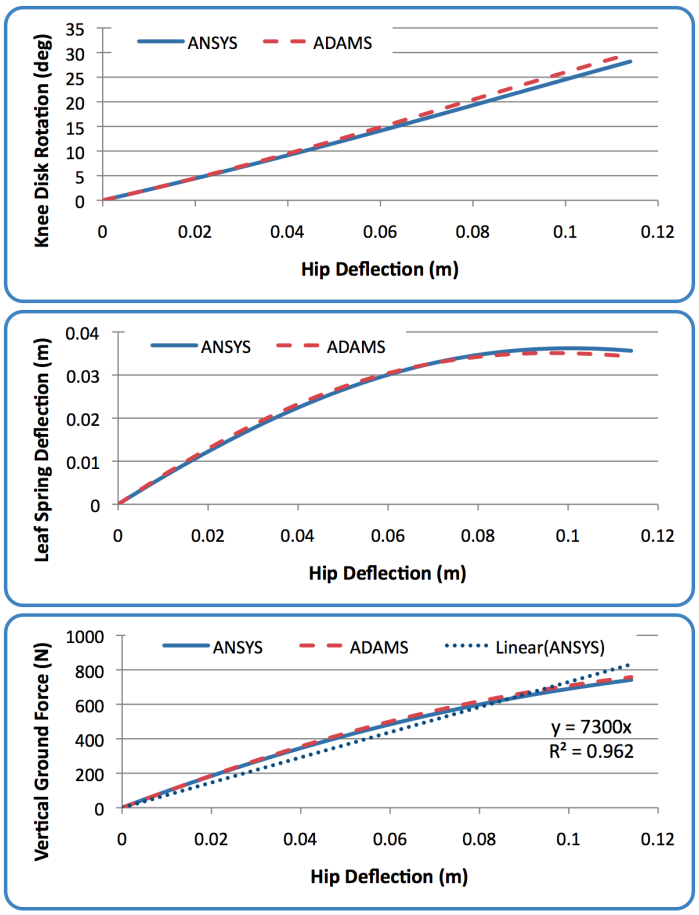

Figure 10. PLOTS OF KNEE DISK ROTATION, LEAF SPRING DEFLECTION, AND VERTICAL GROUND REACTION FORCE FOR BOTH THE SIMPLIFIED ADAMS MODEL AND THE FULL FINITE ELEMENT MODEL. THE ANSYS MODEL VALIDATES THAT THE ADAMS MODEL WAS REASONABLY ACCURATE AND COULD BE USED FOR DESIGN SYNTHESIS AND ITERATION OF SYSTEM DESIGN VARIABLES.

The results shown in the previous section on system modeling used these values. Consequently, the forces, deflections, and stresses shown in those figures are correct for the prototype that was fabricated. For the leaf spring, note that the maximum

stress did not occur at the final time-step shown in Fig. 9; rather, it occurred just beforehand. This is easily seen in Fig. 10 where the leaf spring deformation decreases at the end of hip deflection. Physically this occurred because the vertical force from the applied displacement became less effective as the knee disk rotated according to cosine of the angle of rotation. The stress shown in Fig. 6 of just the leaf spring shows the true maximum stress for the leaf spring.

The material used for the leaf spring was carbon composite in an epoxy matrix. Physical testing of this material showed that typical modulus and fracture strength are 35 GPa and 675 MPa respectively (unpublished results of in-house testing). The maximum stress as seen in Fig. 9 was 483 MPa, yielding a safety factor of 1.4, which is adequate for this application.

The extension spring was also fabricated from carbon composite sheets. Figure 10 above showed that the knee rotation for the ADAMS model underwent a maximum rotation of 30 deg. With the knee disk diameter of 0.053 m, this resulted in a maximum extension spring displacement of 0.029 m and maximum load of 3.32 kN (746 lbf). The purchased pre-fabricated sheets specified a modulus of 45 GPa with a failure stress of 760 MPa. We used closed-form equations to model the tapered cross-section extension spring and verified the results using a nonlinear finite element model (Fig. 11). Maximum stress in the failure analysis was 600 MPa, resulting in a safety factor of 1.3.

2.3.4 Backpack Frame The purpose of the backpack frame was to support the Bowden cable housing at the bottom and the friction-lock and sliding joint at the top. Before knowing the final topology of the frame, we modeled this overall setup quasi-statically in ADAMS as seen in Fig. 12. The loads for this simulation were taken from the system model presented in Sec. 2.3.2. The joints in this model were spring-like bushing elements with stiffness approximately matching the physical system. These elastic elements allowed the loads to be shared between redundant joints even though the system was statically indeterminate. The loads on the joints are shown as red vectors. These loads were extracted from the ADAMS model and applied as the loading condition in the ANSYS finite element model of the backpack frame as seen in Fig. 13.

Table 2. VALUES FOR DESIGN VARIABLES OF ELASTIC ELEMENTS. THESE VALUES WERE OBTAINED BY ITERATING ON THEIR VALUES USING THE ADAMS SYSTEM MODEL UNTIL THE DESIGN OBJECTIVES WERE SATISFIED.

Design Variables	Value
Extension spring stiffness (kN/m)	116
Knee disk diameter (m)	0.053
Resulting torsional stiffness (N-m/deg)	5.77
Spline cross-sectional thickness (mm)	7.62
Spline cross-sectional width (mm)	63.5
Design Objectives	**Value**
Knee disk rotation (deg)	29.8
Exoskeleton stiffness (kN/m)	7.3

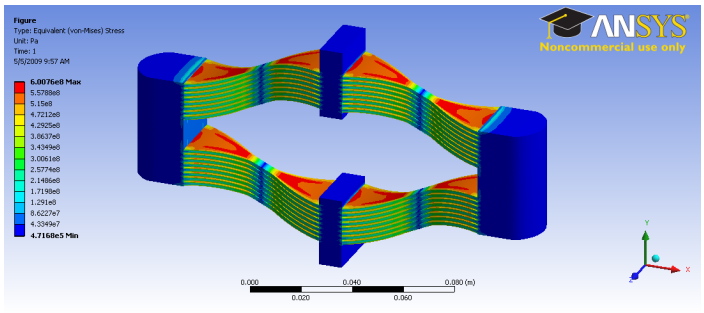

Figure 11. FINITE ELEMENT MODEL OF CARBON COMPOSITE EXTENSION SPRING FOR THE BACKPACK SYSTEM. A TAPERED CROSS-SECTION WAS USED TO EVENLY DISTRIBUTE STRESS AND MINIMIZE MASS.

The goal for backpack frame design was to minimize mass and maximize stiffness. In order to achieve this we used topology optimization with loads determined from the ADAMS analysis. The resulting design is shown in Fig. 13. Because failure due to buckling was a concern in this design, we also performed a buckling analysis. The load multiplier was 2.7 as seen in Fig. 13, meaning that if the load were increased by a factor of 2.7 the frame would buckle. We also performed a static failure analysis comparing the yield strength to the von Mises stress for the frame (Fig. 13 (b)). The minimum safety factor for this analysis was 2.1, indicating that the frame will yield before it buckles and that the device will not fail under the modeled loads.

All other components of the design were similarly analyzed and refined. For each part the goal was to minimize mass while maintaining safety from failure for the given load. Rather than perform detailed optimizations for each component, designs were refined manually. At this stage it was adequate to keep the weight of the device low and quickly design and build a prototype to test the concept of the exoskeleton. Future work will include further design refinement to truly minimize the system mass.

3 PROTOTYPE FABRICATION AND EVALUATION

We fabricated a prototype for one leg of the exoskeleton in order to evaluate the design concept. Only one leg of the exoskeleton was fabricated at this point as the design was not entirely finalized. Table 3 provides weights for individual segments of the prototype and the total mass as calculated for the future two-leg system. Figures 14 and 15 show the prototype in approximately the mid-stance and mid-swing positions. The overall function of

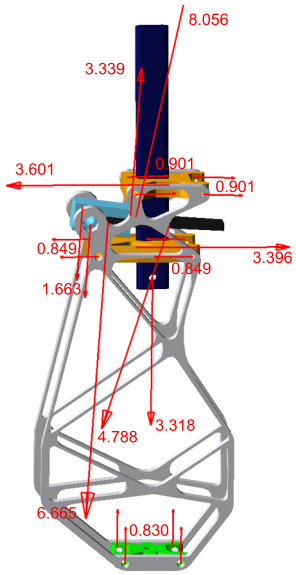

Figure 12. QUASI-STATIC FORCES IN BACKPACK SYSTEM. THESE FORCES OCCUR AT MAXIMUM KNEE DEFLECTION (30 DEG) DURING STANCE AND WERE USED TO DESIGN THE BACKPACK FRAME. THE 3.32 kN FORCE IS THE APPLIED LOAD FROM THE BOWDEN CABLE AND SPRING. THE 0.83, 0.85, AND 1.66 kN LOADS ARE REACTION FORCES ON THE FRAME. THE 8.06, 3.34, 4.79, AND 6.67 kN LOADS ARE BETWEEN COMPONENTS OF THE FRICTION LOCK.

the prototype was described in Sec. 2.2.1 of this paper.

3.1 Quasi-Static Testing

A variety of preliminary tests were performed using this version of the prototype. First we measured the quasi-static performance of the exoskeleton for comparison with modeled behavior. Figure 16 shows the overall stiffness of the exoskeleton. The shallowest curves (in red) are for the original spring as designed and discussed to this point in the paper. As presented in Tab. 4 the actual stiffness of the exoskeleton was much less than predicted. Specifically, the designed stiffness was 7.3 kN/m while the tested stiffness was 3.6 kN/m, roughly half of the predicted

Table 3. MASSES FOR THE PRELIMINARY PROTOTYPE AND ITS SEGMENTS.

Prototype segment	Weight (lbf)	Mass (kg)
Harness	6.8	3.1
Left leg only	5.7	2.6
Backpack system	3.2	1.5
Total for one leg	15.6	7.1
Calculated total for two legs	24.5	11.1

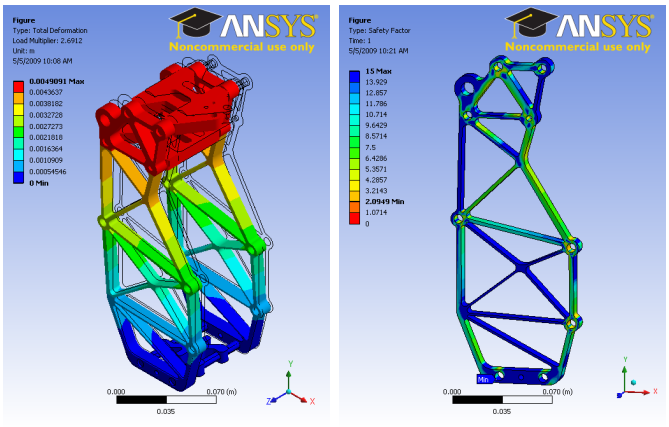

(a) (b)

Figure 13. FINITE ELEMENT MODEL OF THE BACKPACK FRAME USED FOR FAILURE ANALYSIS INCLUDING (a) BUCKLING AND (b) STRESS ANALYSIS. THIS MODEL WAS OPTIMIZED THROUGH TOPOLOGY OPTIMIZATION AND MANUAL DESIGN REFINEMENT TO MINIMIZE THE MASS WHILE MAINTAINING AN ADEQUATE SAFETY FACTOR.

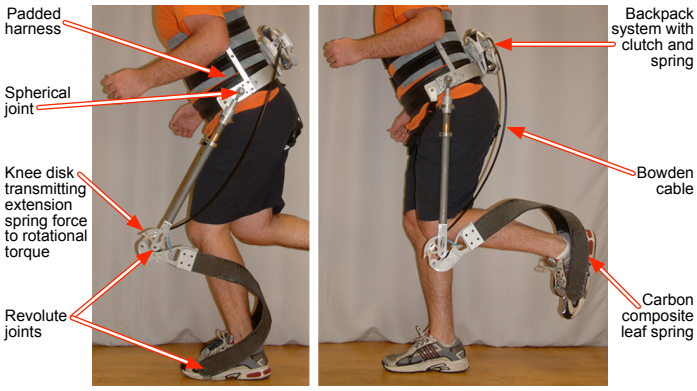

(a) (b)

Figure 14. LATERAL VIEWS OF THE ELASTIC EXOSKELETON IN APPROXIMATELY THE (a) MID-STANCE AND (b) MID-SWING PHASES OF RUNNING.

value. This discrepancy was due to the Bowden cable system and is discussed in conjunction with Fig. 17.

This testing also quantified the energy lost by the exoskeleton system as it was compressed and extended. An ideal spring loses no energy as it compresses and extends to its original length. The shapes of the curves seen in Fig. 16 indicate that there were significant negative work loops, and consequently significant energy loss. When the stiffer spring was used the curves more closely matched the linearized approximation, indicating that the energy loss decreased. When the spring in the back-

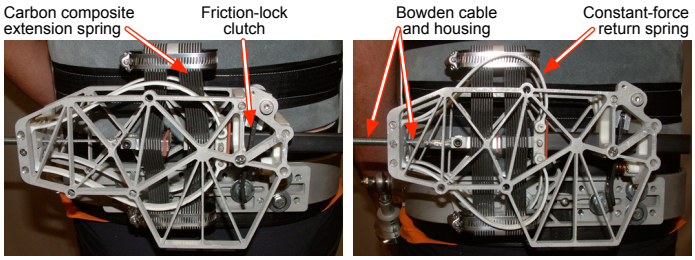

Figure 15. BACKPACK SYSTEM AT (a) MID-STANCE AND (b) MID-SWING PHASES OF RUNNING. NOTE HOW THE COMPOSITE EXTENSION SPRING IS DEFLECTED AT MID-STANCE WHILE THE WHITE PLASTIC RETURN SPRING IS DEFLECTED AT MID-SWING.

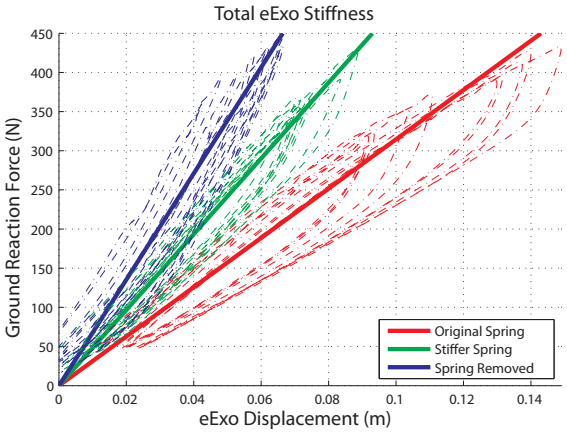

Figure 16. QUASI-STATIC FORCE-DISPLACEMENT TEST RESULTS FOR THE EXOSKELETON. INDIVIDUAL CURVES FOR 10 TRIALS ARE PLOTTED. THE MEAN LINEAR BEST-FIT STIFFNESS FOR EACH CONDITION IS SHOWN IN BOLD. TESTS WERE DONE WITH THE ORIGINAL AND A STIFFER SPRING IN THE BACKPACK AS WELL AS WITH THE BACKPACK SPRING REMOVED.

pack was removed entirely the energy loss decreased even further. These results are summarized in Tab. 4 along with stiffness values.

The energy loss in and decreased stiffness of the exoskeleton system can be attributed to the Bowden cable. In the quasi-static testing above we saw that as the backpack spring stiffness was increased the energy loss decreased. With the stiffness increase came a decrease in cable movement within the housing. Recent research in robotics indicates that Bowden cables are extremely effective at decreasing moving mass but that the friction involved in them can be problematic (see [25] and [26]), as was the case in our elastic exoskeleton. Figure 17 shows the force-deflection behavior of the backpack system tested in isolation on

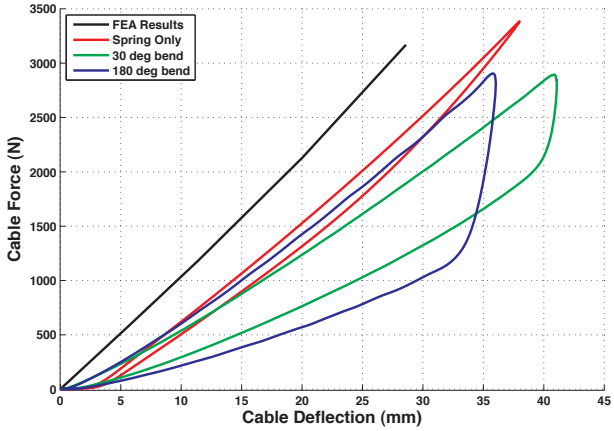

Figure 17. FORCE-DEFLECTION RESULTS FOR THE BACKPACK SPRING SYSTEM. THE BOWDEN CABLE SIGNIFICANTLY AFFECTS THE ENERGY-STORAGE CAPACITY OF THE BACKPACK SYSTEM.

an Instron load frame. When the spring was removed from the backpack and tested by itself, the behavior was fairly close to the FEA results and the energy loss was minimal. However, when the spring was placed in the backpack and the Bowden cable was attached the energy loss went up substantially. This effect became extremely dramatic as the bend in the cable increased (Tab. 5). These curves also demonstrate why the exoskeleton stiffness was significantly less than predicted. Although the slopes of the curves on the loading portion are similar to the FEA model, the cable deflection was substantially higher. This meant that for a given exoskeleton knee rotation the transmitted force was significantly less than desired. Essentially this loss of deflection resulted in an apparent decrease in torsion spring stiffness and explains the decreased stiffness of the exoskeleton system.

In order to ameliorate these losses minor modifications were made to the design. First, the stiffer spring was used rather than the original one. Second, a minor change was made to the cable routing to decrease the total angle through which the Bowden cable was required to bend. As presented in Tab. 4 the stiffness for this modified system was 30% leg stiffness for the preliminary subject and the energy loss was 21%.

Table 5. BACKPACK SYSTEM ENERGY LOSS.

Backpack Setup	Energy Loss Percent (%)
FEA Analysis	0
Spring Only	9
30 deg Bend	34
180 deg Bend	55

Backpack spring	Spring Stiffness (kN/m)	Experimental eExo Stiffness (kN/m)	Percent Leg Stiffness (%)	Energy Loss (%)
Original	111	3.6	22	29
Stiffer	174	4.8	30	21
Removed	N/A	7.6	47	15

Table 4. EXOSKELETON STIFFNESS.

3.2 Control System

The control system for the exoskeleton clutch was very simple. A real-time control system (dSpace, dSPACE Inc., Wixom, MI, USA) received input from an electrogoniometer that measured the hip angle. This signal was filtered and differentiated to yield hip angular velocity. When the sign of the angular velocity changes from positive to negative the control system identified the peak in hip flexion. This event occured just before (∼140 ms for our subject) heel strike. The lag induced by filtering at 6 Hz and the electromechanical delay for engaging the clutch occupy much of this time (∼100 ms in preliminary testing). Consequently the clutch engaged just before heel strike so that the exoskeleton was stiff during the stance phase as it should be. After a fixed time (350 ms) the control signal was sent again. This time delay was chosen so that the actuator attempted to disengage the clutch while the subject was still in the stance phase and the clutch was still under significant load. Because the clutch being used was a friction lock and the actuator was a pneumatic piston that provided a relatively small force, the clutch was not able to release until the system was unloaded. This occurred naturally just before the end of stance phase due to the fact that the toe-hip distance was always shorter at heel-strike than at take-off (see Fig. 19). The clutch was released before the end of stance so that the exoskeleton would provide minimal resistance during leg swing. This behavior is summarized in Fig. 18.

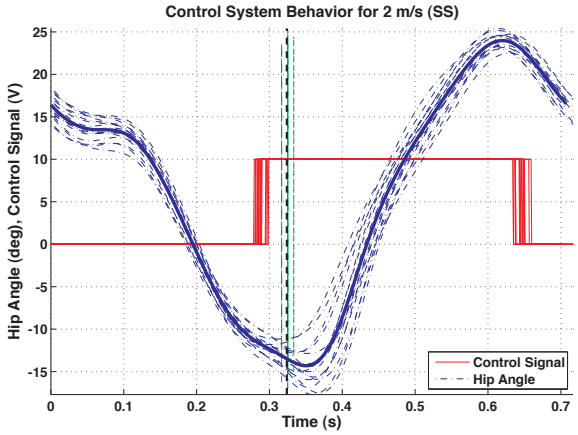

Figure 18. BEHAVIOR OF THE CONTROL SYSTEM FOR THE FRICTION LOCK CLUTCH. INDIVIDUAL CURVES ARE SHOWN FOR 16 STRIDES AND THE MEAN IS PROVIDED IN BOLD LINES. DATA IS PLOTTED FROM LEFT HEEL STRIKE TO LEFT HEEL STRIKE. PEAK HIP FLEXION WAS DETECTED USING AN ELECTROGONIOMETER AT WHICH POINT THE CLUTCH WAS ALLOWED TO ENGAGE (CONTROL SIGNAL DROPS TO ZERO) SUCH THAT THE EXOSKELETON WAS STIFF DURING THE STANCE PHASE. BEFORE THE END OF STANCE (VERTICAL DASHED LINE) THE PNEUMATIC CYLINDER DISENGAGED THE CLUTCH TO ENABLE LEG SWING.

3.3 Exoskeleton Running

The simple control system described in the previous section enabled individuals to run while wearing the exoskeleton. We successfully completed testing of the device on two subjects of similar stature. The results for both subjects were similar so only one set is presented here. The results shown in this section demonstrate the performance and areas for improvement of the elastic exoskeleton. This section is not intended to be an all-inclusive description of human performance while wearing the device. Rather, the focus of this paper is on the design of the device. The human biomechanical results will be presented in a future article. Consequently this section focuses on the high-level description of the exoskeleton's performance while running.

During the stride cycle the exoskeleton successfully modulated from the stiff to the soft behavior. Figure 19(a) shows the force in the exoskeleton as a function of the stride cycle (normalized from left heel strike to left heel strike). During the first half of the plot the force in the exoskeleton develops to a maximum mean value of about 700 N. Recall from Fig. 3 that the subject's leg typically provided ∼2000 N at mid-stance. This means that the exoskeleton provided roughly 35% of the peak force during stance phase. This was slightly higher than our quasi-static testing results indicating that the exoskeleton provides ∼30% of the total leg stiffness with the stiffer spring in the backpack.

Figure 19(b) shows the length of the exoskeleton while running. At heel-strike the exoskeleton was roughly 1.02 m long and at mid-stance it decreased to roughly 0.97 m, or about 5 cm. At toe-off the length was roughly 1.05 m, significantly longer than the length at heel-strike. The secondary joint at the exoskeleton knee allowed the knee to hyper-extend and enabled this increase in length. This also enabled the backpack spring and Bowden cable to become unloaded so that the friction lock could release. During the swing phase, after the vertical dashed line representing toe-off, the exoskeleton length decreased significantly as the

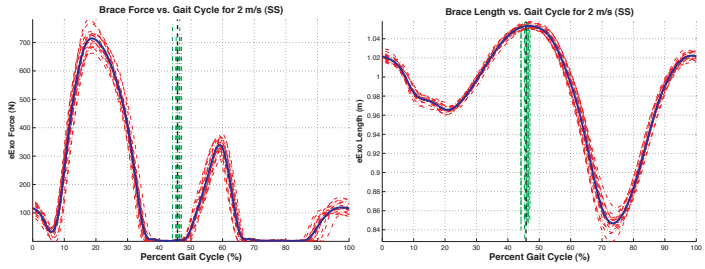

(a) (b)

Figure 19. EXOSKELETON (a) FORCE AND (b) LENGTH DURING THE STRIDE CYCLE. INDIVIDUAL TRIALS ARE SHOWN FOR 16 STRIDES AND THE MEAN IS IN BOLD. THE PLOT BEGINS AND ENDS AT LEFT HEEL-STRIKE; THE VERTICAL DASHED LINE REPRESENTS LEFT TOE-OFF, THE END OF STANCE PHASE.

knee joint was allowed to bend with relatively small resistance. These lengths are slightly higher than those presented in Fig. 2 because the hip attachment point was slightly higher on the waist than assumed in the preliminary design phase.

The resistance provided by the exoskeleton at the beginning of swing phase was the major area for improvement of the device at this point. The resistance will not be zero because some force will always be required to fold up the exoskeleton, or cause it to bend at the knee. Let us refer briefly to this force as the bending force. In this prototype force transmitted at the foot through the shoe provided the bending force. This was quite costly and uncomfortable as the force is applied at the most distal part of the leg. We have since modified the exoskeleton so that a small force is applied on the thigh near the knee via an elastic strap. Applying a bending force proximally decreased the amount of force required and significantly diminished the force peak that occurred just after toe-off. The results of running with the modified system will be presented in a future publication.

This effect was not noticed in the system model because the system was only modeled quasi-statically. Inertial effects of swinging the leg were the major cause of this undesired resistance. When the stance leg swung backwards (hip extension) at the end of stance the exoskeleton thigh segment had a tendency to continue swinging (Newton's 1st Law). The subject's leg started to swing forward for the swing phase but the exoskeleton proceeded backwards towards the kinematic singularity where the hip, knee, and ankle joints were all in a line. As the exoskeleton approached that singularity the force required at the foot to fold up the exoskeleton leg and swing it forward became quite large. This effect was exacerbated when subjects ran at 3.0 m/s.

The small bump in the force at the end of the swing phase just before heel-strike, on the other hand, is not a concern. We believe this force resulted from the exoskeleton leg and harness readjusting as the leg slowed its forward motion in preparation for ground contact. This force was imperceptible to the subjects and was present even while running with the Bowden cable completely disengaged.

4 CONCLUSION

The aim of this design project was to create an elastic exoskeleton to assist human running. Current exoskeletons are constrained by their need for large amounts of power. This is largely due to the inclusion of large motors and bulky structure on the legs. In contrast, the exoskeleton presented in this report is quasi-passive and has a minimal amount of mass on the legs. It relies solely on material deformation or elasticity to store and release energy during the stance phase of running, providing assistance for human running without the need for complex control systems or heavy actuators and power supplies.

A novel knee joint design was implemented in order to achieve a low-profile design with minimal moving mass. This design allowed an extension spring and clutch to be placed on the back where it was relatively inexpensive metabolically to carry. It also provided a torque and rotation at the knee in order to achieve the desired leg stiffness during stance and to more closely follow the shape of the leg both during stance and swing phases of running. Preliminary results while running with the exoskeleton showed that it successfully provided stiffness during stance phase. However, this version of the prototype suffered from significant resistance at the beginning of swing phase due to inertial effects and a kinematic singularity in the exoskeleton.

Future work will present a refined design in which the force at the beginning of leg swing is ameliorated. A second leg will also be included. We will use this device to study human interaction with an elastic exoskeleton while running. In specific we plan to study the effect of elasticity in parallel with the leg on the metabolic cost of running.

5 ACKNOWLEDGEMENTS

This work was supported in part by the National Science Foundation through grant number BES-0347479. Conceptual design and preliminary modeling was done with the assistance of Brandon Chan, Sean Mitera, Philip Dowhan, and Joe Cho. Youngseok Oh provided initial guidance with finite element modeling, Anne Manier and Les Wontorcik assisted with fabrication of the harness and leaf spring, and Evelyn Anaka assisted with data collections.

REFERENCES

[1] Kazerooni, H., Chu, A., and Steger, R., 2007. "That which does not stabilize, will only make us stronger". *International Journal of Robotics Research,* **26**(1), pp. 75–89.

[2] Kawamoto, H., and Sankai, Y., 2005. "Power assist method based on Phase Sequence and muscle force condition for HAL". *Advanced Robotics,* **19**(7), pp. 717–734.

[3] Jacobsen, S. C., Olivier, M., Smith, F. M., Knutti, D. F., Johnson, R. T., Colvin, G. E., and Scroggin, W. B., 2004. "Research robots for applications in artificial intelligence, teleoperation and entertainment; high performance robots; teleoperation; exoskeleton; entertainment". *International Journal of Robotics Research,* **23**(4-5), pp. 319–330.

[4] Farley, C. T., and Ferris, D. P., 1998. "Biomechanics of walking and running: center of mass movements to muscle action". *Exercise and Sport Sciences Reviews,* **26**(1), January, pp. 253–285.

[5] Sawicki, G. S., Lewis, C. L., and Ferris, D. P., 2009. "It pays to have a spring in your step". *Exercise and Sport Sciences Reviews*(In press).

[6] Alexander, R. M., 1990. "Three uses for springs in legged locomotion". *The International Journal of Robotics Research,* **9**(2), April, pp. 53–61.

[7] Pratt, J. E., Krupp, B. T., and Collins, S. H., 2004. "The RoboKnee: an exoskeleton for enhancing strength and endurance during walking". *Proceedings of the IEEE International Conference on Robotics & Automation*, April, pp. 2430–2435.

[8] Low, K. H., Liu, X., and Yu, H., 2006. "Design and implementation of NTU wearable exoskeleton as an enhancement and assistive device". *Applied Bionics and Biomechanics,* **3**(3), pp. 209–25.

[9] Walsh, C. J., Paluska, D., Pasch, K., Grand, W., Valiente, A., and Herr, H., 2006. "Development of a lightweight, underactuated exoskeleton for load-carrying augmentation". In 2006 Conference on International Robotics and Automation, Proceedings, IEEE, pp. 3485–91.

[10] Carr, C. E., and Newman, D. J., 2008. "Characterization of a lower-body exoskeleton for simulation of space-suited locomotion". *Acta Astronautica,* **62**(4-5), pp. 308–323.

[11] Banala, S. K., Agrawal, S. K., Fattah, A., Krishnamoorthy, V., Hsu, W.-L., Scholz, J., and Rudolph, K., 2006. "Gravity-balancing leg orthosis and its performance evaluation". *IEEE Transactions on Robotics,* **22**(6), December, pp. 1228–1239.

[12] Herder, J., 2001. *Energy-free Systems. Theory, conception and design of statically balanced spring mechanisms*. ISBN 90-370-0192-0.

[13] Dollar, A. M., and Herr, H., 2008. "Design of a quasi-passive knee exoskeleton to assist running". *IEEE International Conference on Intelligent Robots and Systems*, pp. 747–754.

[14] Dollar, A. M., and Herr, H., 2008. "Lower extremity exoskeletons and active orthoses: Challenges and state-of-the-art". *IEEE Transactions on Robotics,* **24**(1), pp. 144–158.

[15] Blickhan, R., 1989. "The spring-mass model for running and hopping". *Journal of Biomechanics,* **22**(11/12), pp. 1217–1227.

[16] McMahon, T. A., and Cheng, G. C., 1990. "The mechanics of running: how does stiffness couple with speed?". *Journal of Biomechanics,* **23**(Suppl. 1), pp. 65–78.

[17] McGeer, T., 1990. "Passive bipedal running". *Proceedings of the Royal Society of London, B, Biological Sciences,* **240**(1297), pp. 107–134.

[18] Alexander, R. M., 1992. "A model of bipedal locomotion on compliant legs.". *Philosophical transactions of the Royal Society of London. Series B: Biological sciences,* **338**(1284), pp. 189–198.

[19] Geyer, H., Seyfarth, A., and Blickhan, R., 2006. "Compliant leg behaviour explains basic dynamics of walking and running.". *Proc Biol Sci,* **273**(1603), November, pp. 2861–2867.

[20] O'Connor, S. M., and Kuo, A. D., 2007. "Walking, skipping, and running produced from a single bipedal model". In Proceedings of the American Society of Biomechanics Annual Conference.

[21] Whittington, B. R., and Thelen, D. G., 2009. "A simple mass-spring model with roller feet can induce the ground reactions observed in human walking.". *J Biomech Eng,* **131**(1), February, p. 011013.

[22] Ferris, D. P., Bohra, Z. A., Lukos, J. R., and Kinnaird, C. R., 2006. "Neuromechanical adaptation to hopping with an elastic ankle-foot orthosis". *Journal of Applied Physiology,* **100**(1), January, pp. 163–170.

[23] Cherry, M. S., Choi, D. J., Deng, K. J., Kota, S., and Ferris, D. P., 2006. "Design and fabrication of an elastic knee orthosis — preliminary results". *Proceedings of the ASME International Design Engineering Technical Conferences*(2006-99622), September.

[24] Browning, R. C., Modica, J., Kram, R., and Goswami, A., 2007. "The effects of adding mass to the legs on the energetics and biomechanics of walking". *Medicine & Science in Sports & Exercise,* **39**(3), pp. 515–525.

[25] Schiele, A., 2008. "Performance difference of bowden cable relocated and non-relocated master actuators in virtual environment applications". *Proceedings of the IEEE International Conference on Intelligent Robots & Systems*, pp. 3507–3512.

[26] Veneman, J. F., Ekkelenkamp, R., Kruidhof, R., van der Helm, F. C. T., and van der Kooij, H., 2006. "A series elastic- and bowden-cable-based actuation system for use as torque actuator in exoskeleton-type robots". *I. J. Robotic Res.,* **25**(3), pp. 261–281.